Imaging Intracellular Viscosity of a Single Cell During Photoinduced Cell Death

Marina K. Kuimova,[1,5] Stanley W. Botchway,[2] Anthony W. Parker,[2] Milan Balaz,[3] Hazel A. Collins,[3] Harry L. Anderson,[3] Klaus Suhling[4] and Peter R. Ogilby[5*]*

[1] Chemistry Department, Imperial College London, Exhibition Road, SW7 2AZ, UK

[2] Central Laser Facility, Science and Technology Facilities Council, Rutherford Appleton Laboratory, Harwell Science and Innovation Campus, Didcot, Oxfordshire, OX11 0QX, UK

[3] Oxford University, Department of Chemistry, Chemistry Research Laboratory, Oxford, OX1 3TA, UK

[4] Department of Physics, King's College London, Strand, London WC2R 2LS, UK

[5] Center for Oxygen Microscopy and Imaging (COMI) , Department of Chemistry, University of Aarhus, Århus DK-8000, Denmark

E-MAIL: m.kuimova@imperial.ac.uk progilby@chem.au.dk

Diffusion mediated cellular processes, such as metabolism, signaling and transport depend on the hydrodynamic properties of the intracellular matrix. Photodynamic therapy, used in the treatment of cancer, relies on the generation of short-lived cytotoxic agents within a cell upon irradiation of a drug. The efficacy of this treatment depends on the viscosity of the medium through which the cytotoxic agent must diffuse. Here, spectrally resolved fluorescence measurements of a porhyrin dimer-based molecular rotor are used to quantify intracellular viscosity changes in single cells. We show that there is a dramatic increase in viscosity of the immediate environment of the rotor upon photoinduced cell death. The effect of this viscosity increase is directly observed in the diffusion-dependent kinetics of the photosensitized formation and decay of a key cytotoxic agent, singlet molecular oxygen. Using these tools we provide insight into the dynamics of diffusion in cells, which is pertinent to drug delivery, cell signaling and intracellular mass transport.

Diffusion-mediated cellular processes, such as metabolism, signaling and transport, depend on the hydrodynamic properties of the intracellular matrix. The translational diffusion coefficient (D) for a given intracellular solute depends on the fluid phase viscosity of the cytoplasm as well as on collisions and interactions that occur between the solute and intrinsic cellular macromolecules.[1] Values of D for both small solutes[1-5] and macromolecules[6,7] in mammalian cells can be 5-50 times smaller than those in pure water. Recent measurements in cell vesicles[8] demonstrated that the local microviscosity can be as high as 140 cP, while the microviscosity in the aqueous phase of the cellular cytoplasm is several cP, similar to that of pure water.[9-11] Such large viscosity variations within a cell can influence diffusion and bimolecular reaction rates,[12] and need to be considered, for example, while developing strategies for drug delivery and cancer therapy.

Fluorescent molecular rotors, in which the non-radiative decay of an excited state can be altered by the ambient viscosity, have emerged as a new modality for measuring the microviscosity in a biological environment.[8,13,14] This approach complements viscosity-dependent fluorescence depolarization work, pioneered by Perrin[15] and Weber.[16] Precise calibration of the rotor response to viscosity can be achieved by either using fluorescence lifetime-based measurements[8] or a ratiometric approach.[14] The current work uses a new type of rotor, constructed as a conjugated porphyrin dimer (**1**, Fig. 1). Recently, the remarkable non-linear optical properties of **1**, together with its high intracellular uptake, photostability and favorable photophysical properties, have been exploited to create an efficient photosensitizer for one-photon and two-photon excited photodynamic therapy (PDT) of cancer.[17-20] In PDT, cell death and tissue eradication is achieved upon irradiation of the photosensitizer and the subsequent production of cytotoxic species, in particular

singlet molecular oxygen, $O_2(a^1\Delta_g)$, Fig. 1b.[21] Now, by utilizing the properties of dimer **1** as both a PDT photosensitizer and a fluorescent ratiometric molecular rotor we (i) initiate cell death *via* irradiation of **1**, and (ii) monitor changes in the intracellular viscosity of light-perturbed single cells. Finally, we illustrate the effect of the light-induced viscosity change on intracellular diffusion and reaction rates by direct time-resolved single-cell spectroscopic studies of $O_2(a^1\Delta_g)$, monitoring its formation and decay rates with subcellular resolution.

Results

The Molecular Rotor

The spectroscopic properties of a butadiyne-linked porphyrin dimer, structurally related to **1**, have been described in terms of two conformations: planar and twisted, referring to the relative position of the porphyrin units.[22] Each conformer is characterized by distinctive absorption and emission spectra. The emission of the dimer in fluid solution was dominated by the lower energy planar conformation, whereas the emission of the less stable twisted conformer could be observed from glassy matrices where rotation of the two porphyrin units relative to each other is restricted.

The absorption and emission spectra for **1** in solutions of varying viscosity, ranging from 0.6 to 950 cP, are shown in Fig. 1 and Fig. 2a. The spectral changes that occur with an increase in viscosity are consistent with the formation of increasing amounts of the twisted conformer of **1**,[22] as torsional rotation about the butadiyne link becomes slower in viscous media. Thus, we assign the emission maximum of **1** at 710 nm to the twisted conformation and the emission maximum at 780 nm to the planar conformation.

The calibration of the viscosity-dependent rotor response of **1** following 473 nm excitation using a ratiometric approach is shown in Fig. 2a (inset). The plot of the intensity ratio of the two fluorescence peaks of **1** against viscosity in double logarithmic coordinates shows a good linear correlation, as expected from theory.[23]

Dimer **1** is efficiently incorporated into live cells.[19] The fluorescence spectrum of **1** in a cell, Fig. 2b, clearly shows two well-resolved maxima at *ca.* 710 and 780 nm, corresponding to emission from the twisted and planar conformations of the dimer, respectively. Using the viscosity calibration graph (Fig. 2a inset), we ascertain that the viscosity of the intracellular compartments where **1** localizes is *ca*. 50 cP, see supplementary information. A similarly high viscosity was reported for endocytotic vesicles of live cells.[8]

The fluorescence spectrum of **1** was also recorded in the bulk cell culture medium. Here, the emission spectral shape shows only a slight deviation from that in non-viscous solutions, Fig. 2a. The small increase in apparent viscosity measured by **1** in the culture medium compared to methanol corresponds to the surface binding of **1** to Bovine Serum Albumin (BSA), as previously established for a series of ionic dimers similar to **1**[19] and smaller charged porphyrins.[24,25] Since the dimer **1** is too large for highly specific 'lock-key' binding with intracellular proteins,[26] which can significantly restrict its conformational dynamics, the spectrum of intracellular **1** must reflect a large ambient viscosity, not specific binding. This point is corroborated by the independent singlet oxygen experiments, *vide infra*.

An important advantage of monitoring intracellular microviscosity using molecular rotors is the possibility to characterize a dynamically changing environment. We illustrate

this by recording emission spectra of **1** inside cells during PDT, *i.e.* irradiation with light which ultimately results in cell death, Fig. 2c.

Upon irradiation with light, **1** sensitizes the production of cytotoxic $O_2(a^1\Delta_g)$[19] (Fig. 1b) and initiates cell death.[17,20] The series of emission spectra obtained upon irradiation of **1** in a single cell, Fig. 2c, correspond to a significant increase in the viscosity of the intracellular environment surrounding **1**. Importantly, the spectrum obtained for **1** in a cell culture medium does not change shape upon 473 nm irradiation, Fig. 2c (inset), suggesting that the behavior observed for **1** in a cell is not a result of binding to proteins. Using the calibration graph (Fig. 2a inset), we determine the post-PDT viscosity of the cellular domains containing **1** as (300±50) cP. This value is significantly greater than that obtained prior to PDT (*vide supra*). Such a viscosity increase likely reflects cross linking reactions, mediated by singlet oxygen or secondary reactive radicals, similar to those observed in model and intracellular protein systems.[27-30]

Singlet Oxygen Experiments

Increased viscosity can alter the rate of many diffusion-dependent processes in a cell. We set out to establish the effect of the photoinduced change in intracellular viscosity on the kinetics of photosensitized formation and decay of cytotoxic $O_2(a^1\Delta_g)$. It has been demonstrated that in spite of an extremely low quantum yield of its emission, *ca.* 10^{-6}, $O_2(a^1\Delta_g)$ can be monitored by its 1270 nm phosphorescence in single cells.[31,32] Fig. 3a shows averaged $O_2(a^1\Delta_g)$ phosphorescence traces recorded at 1270 nm after excitation of **1** in cells. The two traces were obtained from the same cell location upon initial and prolonged irradiation. The observed irradiation-dependent decrease in the rate of signal decay, from $(16 \pm 2\ \mu s)^{-1}$ to $(28 \pm 3\ \mu s)^{-1}$, suggests an increase in the viscosity of the

environment where $O_2(a^1\Delta_g)$ has been produced, with a corresponding decrease in the rate of bimolecular quenching,[12] see supplementary information.

5,10,15,20-Tetrakis(*N*-methyl-4-pyridyl)-21*H*,23*H*-porphine (TMPyP, **2**) is a well-studied $O_2(a^1\Delta_g)$ sensitizer.[12,31,32] We now turn to using TMPyP to investigate the effect of irradiation-induced viscosity changes on $O_2(a^1\Delta_g)$ kinetics. The 1270 nm $O_2(a^1\Delta_g)$ traces recorded as a function of elapsed irradiation time of intracellular TMPyP are shown in Fig. 3b. The data clearly show irradiation-dependent decreases in both the rate of signal decay, from $(23.7 \pm 0.8\ \mu s)^{-1}$ to $(30 \pm 1\ \mu s)^{-1}$, and in the rate of signal formation, from $(<<1\ \mu s)^{-1}$ to $(6 \pm 1\ \mu s)^{-1}$. These changes are consistent with an increase in viscosity that influences bimolecular events resulting in (i) $O_2(a^1\Delta_g)$ formation *i.e.* triplet state sensitizer deactivation by oxygen and (ii) $O_2(a^1\Delta_g)$ decay *i.e.*, collisions with intracellular quenchers.

These irradiation-induced changes in the $O_2(a^1\Delta_g)$ phosphorescence signals occur on approximately the same time scale of elapsed irradiation as the fluorescence spectral change of the molecular rotor (Fig. 2c inset). The coincidence of these time scales and the fact that we observe a change in both triplet deactivation and singlet oxygen lifetimes, allows us to rule out the depletion of oxygen in the local environment of the photosensitizer as a reason for the observed changes in the time resolved 1270 nm signals. In fact, the integrated intensity of the $O_2(a^1\Delta_g)$ phosphorescence signal increases as irradiation time elapses, suggesting an increase, not a decrease, in the local oxygen concentration. The latter would be observed if $O_2(a^1\Delta_g)$ was produced in hydrocarbon-dominated domains where the solubility of oxygen is much higher than in aqueous phase,[33] which is consistent with

photo-initiated cross linking leading to intracellular domains of high viscosity. In short, PDT treatment of cells indeed results in the viscosity-dependent decrease of the diffusion and bimolecular reaction rates of species in a cell.

Imaging Intracellular Viscosity Changes

In the highly heterogeneous environment of a viable cell, it is particularly attractive to obtain a spatially resolved image of intracellular viscosity. Here we use the spectrally resolved fluorescence measurements of **1** to obtain ratiometric viscosity maps of a cell as a function of elapsed irradiation time (Fig. 4). These images clearly show that the intracellular viscosity is inhomogeneous and that intracellular viscosity increases during irradiation.

Discussion

We report a new type of ratiometric fluorescent molecular rotor suitable for quantifying and imaging of intracellular viscosity in live cells. The rotor enables real-time monitoring of dynamic processes in cells. The latter has been illustrated by quantifying a significant increase in intracellular viscosity during photoinduced cell death. We also demonstrated that such a viscosity increase indeed alters diffusion-dependent kinetics in a cell, illustrated through changes in the photosensitized production and subsequent decay of the cytotoxic species, singlet oxygen, $O_2(a^1\Delta_g)$. A major challenge of studying dynamic biological systems is that one must constantly consider phenomena that alter the heterogeneous sub-micron environment of a cell. In this report, we have presented tools that will help to unravel the underlying mechanisms of such processes.

Methods

The viscosity of the methanol/glycerol mixtures at 22 ºC was measured as described previously,[8] see supplementary information.

The Chinese Hamster Ovarian carcinoma (CHO) and HeLa cell lines were obtained from the European Collection of Cell Cultures (ECACC). Cells were cultured in Dulbecco's modified Eagle's medium (DMEM) with 10% foetal calf serum (FCS), penicillin and streptomycin antibiotics and passaged when 70-90% confluent in 10 cm^3 flasks grown at 37ºC in 5% CO_2. For fluorescence imaging, cells were seeded at 10^4 cells/well in 0.2 ml of culture medium in untreated 8-well coverglass chambers (Lab-Tek^{TM}, Nunc) and allowed to grow to confluence for 24 h. The culture medium was replaced with the culture medium containing 10 μM of **1** or TMPyP and incubated for 20 hours. To facilitate incorporation of **1**, the culture medium for incubation was prepared by dilution from 1.0 mM stock of **1** in DMSO. Following incubation, the chambers were washed twice with phosphate buffer saline (PBS) and images taken at 22°C. The CHO cell line was used in all experiments with **1**. The HeLa cell line was used in all experiments with TMPyP. Under our experimental conditions, **1** localizes in the cell cytoplasm[19] and TMPyP localizes in the cell nucleus and the cytoplasm.[12, 31, 32] Upon excitation of TMPyP, the fluorescence and singlet oxygen signals can be detected independently from both cell locations.

Fluorescence cell imaging was performed by irradiating the entire cell and its surroundings with a steady-state Xe lamp using interference filters to select the appropriate excitation wavelength. Light emitted by the sample was detected through interference filters using a CCD camera (Evolution QEi controlled by ImagePro software, Media Cybernetics) placed at the image plane of the microscope. Bright-field images were

recorded using the same CCD camera, and back-lighting was achieved with a tungsten lamp provided as an accessory to an Olympus IX70 inverted microscope using an oil-immersion 100× objective (NA = 1.30). The ratiometric images were obtained in ImageJ software, see supplementary information.

The fluorescence spectra of **1** from cells were obtained using 473 nm pulsed excitation from a diode laser (Becker&Hickl, BDL-473-SMC, 10 mW, 20 MHz) coupled to a microscope. The output power was attenuated using neutral density filters to < 0.1 mW. The emission was spectrally dispersed using a spectrograph monochromator (Acton, spectradrive 275) in the range between 500 and 800 nm and detected using a CCD (Andor iDus BU440). The CCD was calibrated using the output of a low pressure mercury lamp (435, 546, 579 and 706 nm) and a HeNe laser (633 nm).

For singlet oxygen detection, cells to be studied were contained in an atmosphere-controlled chamber that was mounted onto the translation stage of an inverted microscope. The sensitizer that had been incorporated into the cell was irradiated using the output of a femtosecond laser system through the microscope objective (Olympus, IR coating, 60×, NA=0.90, irradiated spot size ~1 μm diameter). The emitted light was collected using the microscope objective, spectrally isolated using an interference filter (1270 ± 15) nm, and transmitted to a cooled photomultiplier tube, operated in a photon counting mode, coupled to a multiscaler (MSA 300, Becker & Hickl), see supplementary information. In a typical experiment, excitation energies ranged from 3 to 10 nJ/pulse at a repetition rate of 1 kHz. These experiments were performed using cells exposed to an atmosphere of 100 % oxygen, which results in the most intense $O_2(a^1\Delta_g)$ phosphorescence signal.[5,32] During incubation, the H_2O-based DMEM medium was exchanged with a D_2O-based medium, as previously

described.[31] This procedure results in a larger quantum efficiency of singlet oxygen emission, and has no ill effects on the viability of the cells over the time course of our experiments.[31]

References

[1] Kao, H.P., Abney, J.R., and Verkman, A.S., Determinants of the translational mobility of a small solute in cell cytoplasm. *J. Cell Biol.* **120** (1), 175 (1993).

[2] Jones, D. P., Effect of mitochondrial clustering in O_2 supply in hepatocytes. *Am. J. Phisiol.* **247** (1), C83 (1984).

[3] O'Loughlin, M.A., Whillans, D.W., and Hunt, J.W., A fluorescence approach to testing the diffusion of oxygen into mammalian cells. *Radiat. Res.* **84** (3), 477 (1980).

[4] Uchida, K., Matsuyama, K., Tanaka, K., and Doi, K., Diffusion coefficient for O_2 in plasma and mitochondrial membranes of rat cardiomyocytes. *Respiration Physiology* **90** (3), 351 (1992).

[5] Hatz, S., Poulsen, L., and Ogilby, P.R., Time-resolved singlet oxygen phosphorescence measurements from photosensitized experiments in single cells: the effect of oxygen diffusion and oxygen concentration. *Photochem. Photobiol.* **84** (5), 1284 (2008).

[6] Wojcieszyn, J.W., Schlegel, R.A., Wu, E.S., and Jacobson, K.A., Diffusion of injected macromolecules within the cytoplasm of living cells. *Proc. Natl. Acad. Sci. U. S. A.* **78** (7), 4407 (1981).

[7] Seksek, O., Biwersi, J., and Verkman, A.S., Translational diffusion of macromolecule-sized solutes in cytoplasm and nucleus. *J. Cell Biol.* **138** (1), 131 (1997).

[8] Kuimova, M.K., Yahioglu, G., Levitt, J.A., and Suhling, K., Molecular rotor measures viscosity via fluorescence lifetime imaging. *J. Am. Chem. Soc.* **130** (21), 6672 (2008).

[9] Dix, J.A. and Verkman, A.S., Mapping of fluorescence anisotropy in living cells by ratio imaging - application to cytoplasmic viscosity. *Biophys. J.* **57** (2), 231 (1990).

[10] Luby-Phelps, K. et al., A novel fluorescence ratiometric method confirms the low solvent viscosity of the cytoplasm. *Biophys. J.* **65** (1), 236 (1993).

[11] Suhling, K. et al., Time-resolved fluorescence anisotropy imaging applied to live cells. *Opt. Lett.* **29** (6), 584 (2004).

[12] Kuimova, M.K., Yahioglu, G., and Ogilby, P.R., Singlet Oxygen in a Cell: Spatially-Dependent Lifetimes and Quenching Rate Constants. *J. Am. Chem. Soc.* DOI: 10.1021/ja807484b (2009).

[13] Haidekker, M.A. and Theodorakis, E.A., Molecular rotors - fluorescent biosensors for viscosity and flow. *Org. Biomol. Chem.* **5** (11), 1669 (2007).

[14] Haidekker, M.A., Brady, T.P., Lichlyter, D., and Theodorakis, E.A., A ratiometric fluorescent viscosity sensor. *J. Am. Chem. Soc.* **128** (2), 398 (2006).

[15] Perrin, F., La fluorescence des solutions: induction moleculaire. Polarisation et duree d'emission. Photochimie. *Ann. Phys.* **12**, 169 (1929).

[16] Shinitzky, M., Dianoux, A.C., Gitler, C., and Weber, G., Microviscosity and order in the hydrocarbon region of micelles and membranes determined with fluorescent probes. I. Synthetic micelles. *Biochemistry* **10** (11), 2106 (1971).

[17] Collins, H.A. et al., Blood vessel closure using photosensitisers engeneered for two-photon excitation. *Nature Photonics* **2**, 420 (2008).

[18] Balaz, M., Collins, H.A., Dahlstedt, E., and Anderson, H.L., Synthesis of biocompatible conjugated porphyrin dimers for one-photon and two-photon excited photodynamic therapy at NIR wavelengths. *Org. Biomol. Chem.* **in press**, DOI: 10.1039/b814789b (2009).

[19] Kuimova, M.K. et al., Photophysical Properties and Intracellular Imaging of Water-Soluble Porphyrin Dimers for Two-Photon Excited Photodynamic Therapy. *Org. Biomol. Chem.* **in press**, DOI: 10.1039/b814791d (2009).

[20] Dahlstedt, E. et al., One- and two-photon activated phototoxicity of conjugated porphyrin dimers with high two-photon absorption cross-sections. *Org. Biomol. Chem.* **in press**, DOI: 10.1039/b814792b (2009).

[21] Bonnett, R., *Chemical Aspects of Photodynamic Therapy*. (Gordon and Breach Science Publishers, Amsterdam, 2000).

[22] Winters, M.U. et al., Photophysics of a butadiyne-linked porphyrin dimer: Influence of conformational flexibility in the ground and first singlet excited state. *J. Phys. Chem. C* **111** (19), 7192 (2007).

[23] Förster, T. and Hoffmann, G., Viscosity dependence of fluorescent quantum yields of some dye systems. *Z. Phys. Chem.* **75** (1-2), 63 (1971).

[24] Borissevitch, I.E., Tominaga, T.T., and Schmitt, C.C., Photophysical studies on the interaction of two water-soluble porphyrins with bovine serum albumin. Effects upon the porphyrin triplet state characteristics. *J. Photochem. Photobiol., A* **114** (3), 201 (1998).

[25] Lang, K., Mosinger, J., and Wagnerova, D.M., Photophysical properties of porphyrinoid sensitizers non-covalently bound to host molecules; models for photodynamic therapy. *Coord. Chem. Rev.* **248** (3-4), 321 (2004).

[26] Zunszain, P.A., Ghuman, J., Komatsu, T., Tsuchida, E., and Curry, S., Crystal structural analysis of human serum albumin complexed with hemin and fatty acid. *BMC Struct. Biol.* **3**, 6 (2003).

[27] Goosey, J.D., Zigler, J.S., and Kinoshita, J.H., Cross-linking of lens crystallins in a photodynamic system - a process mediated by singlet oxygen. *Science* **208** (4449), 1278 (1980).

[28] Dubbelman, T., Degoeij, A., and Vansteveninck, J., Photodynamic effects of Protoporphyrin on human erythrocytes - a nature of cross-linking of membrane proteins. *Biochim. Biophys. Acta* **511** (2), 141 (1978).

[29] Verweij, H., Dubbelman, T., and Vansteveninck, J., Photodynamic protein cross-linking. *Biochim. Biophys. Acta* **647** (1), 87 (1981).

[30] Basu, S., Rodionov, V., Terasaki, M., and Campagnola, P.J., Multiphoton-excited microfabrication in live cells via Rose Bengal cross-linking of cytoplasmic proteins. *Opt. Lett.* **30** (2), 159 (2005).

[31] Hatz, S., Lambert, J.D.C., and Ogilby, P.R., Measuring the lifetime of singlet oxygen in a single cell: addressing the issue of cell viability. *Photochem. Photobiol. Sci.* **6**, 1106 (2007).

[32] Snyder, J.W., Skovsen, E., Lambert, J.D.C., and Ogilby, P.R., Subcellular, time-resolved studies of singlet oxygen in single cells. *J. Am. Chem. Soc.* **127** (42), 14558 (2005).

[33] *Oxygen and Ozone*. R. Battino, Ed., Solubility Data Series (Pergamon Press, Oxford, 1981), vol. 7.

Supplementary information accompanies this paper at www.nature.com/naturechemistry

Acknowledgements. MKK is thankful to the EPSRC Life Sciences Interface programme for a personal fellowship. We thank STFC for funding access to the Central Laser Facility. This work was supported in part by the Danish National Research Foundation under a block grant for the Center for Oxygen Microscopy and Imaging. Correspondence and requests for material should be addressed to MKK and PRO.

Author Contributions. MKK designed the research, MKK, SWB and AWP measured fluorescence spectra, MKK performed ratiometric imaging and measured singlet oxygen traces. MB and HAC synthesized the porphyrin dimer. All authors discussed the results and contributed to the manuscript.

Figure captions

Figure 1. (a) Structure of the porphyrin-dimer-based rotor **1**; (b) a schematic representation of one-photon photosensitized singlet oxygen production: irradiation of the sensitizer (e.g., **1**) populates a singlet excited state, S_1; intersystem crossing from S_1 produces a long-lived triplet state, T_1; energy transfer from T_1 to ground state oxygen, $O_2(X^3\Sigma_g^-)$, generates singlet oxygen; (c) absorption spectra of **1** in methanol/glycerol mixtures of increasing viscosity, from 0.6 cP (methanol, red line) to 950 cP (95% glycerol, black line). The changes in absorption are consistent with the formation of increasing amounts of the twisted conformer of **1** in more viscous media.

Figure 2. Emission spectra obtained upon 473 nm excitation of **1** in solution and in cells. (a) In methanol/glycerol mixtures of different viscosity; inset: double logarithmic plot of the intensity ratio of the emission peaks at 710 nm and 780 nm *vs* the solution viscosity. The changes in emission are consistent with the formation of increasing amounts of the twisted conformer of **1** in more viscous media and this makes ratiometric viscosity calibration possible; (b) in a cell (black) and in the bulk culture medium supplemented with 10% FCS (red); (c) in a cell recorded as a function of time following irradiation at 473 nm (0.1 mW, 1 min/spectrum); inset: the intensity ratio of the emission peaks at 710 nm and 780 nm *vs* irradiation time in a cell (black) and in the culture medium, ×3 (red). The intracellular intensity ratio increases following irradiation corresponding to a significant increase in local microviscosity.

Figure 3. Time-resolved singlet oxygen phosphorescence traces recorded at 1270 nm from D_2O-incubated cells. (a) Signals produced upon 790 nm irradiation of **1** in a cell: (■) the trace obtained in the first 3 min of irradiation, (○) the trace obtained from the same cell location in a subsequent 3 min period. Traces are offset for clarity, and each was obtained by averaging measurements from 5 cells; (b) Signals produced upon 420 nm irradiation of TMPyP (**2**) in a single location of a cell over three subsequent periods of 3 min irradiation. The structure of TMPyP is also shown.

Figure 4. Imaging the change in the intracellular viscosity using **1** *via* the ratiometric approach. The transmission (a) and ratiometric fluorescence images of **1** (b, c) in a cell (λ_{ex} = 480±15 nm) obtained during initial (b) and advanced (c) stages of irradiation; blue corresponds to lower viscosity, orange to higher viscosity, and all viscosities are in the range >> 1 cP. The ratiometric images were obtained from conventional fluorescence intensity images (d-f) using ImageJ software. The intensity image with λ_{det} = 700±20 nm (e, f) recorded either in the initial (e) or advanced (f) stages of irradiation was divided by the intensity image with λ_{det} = 800±20 nm (d). Image (d) remained unchanged during irradiation. The changes from (b) to (c) and from (e) to (f) demonstrate that the intracellular viscosity increases during irradiation.

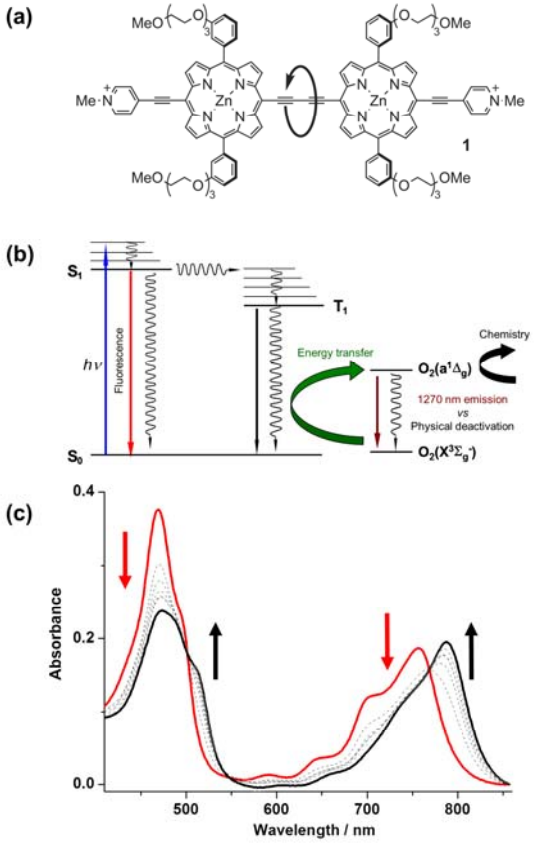
(a)
MeO
OMe
Me·N
N·Me
Zn
1
(b)
S1
T1
hν
Fluorescence
Energy transfer
Chemistry
O2(a1Δg)
1270 nm emission
vs
Physical deactivation
S0
O2(X3Σg-)
(c)
Absorbance
0.4
0.2
0.0
500
600
700
800
Wavelength / nm

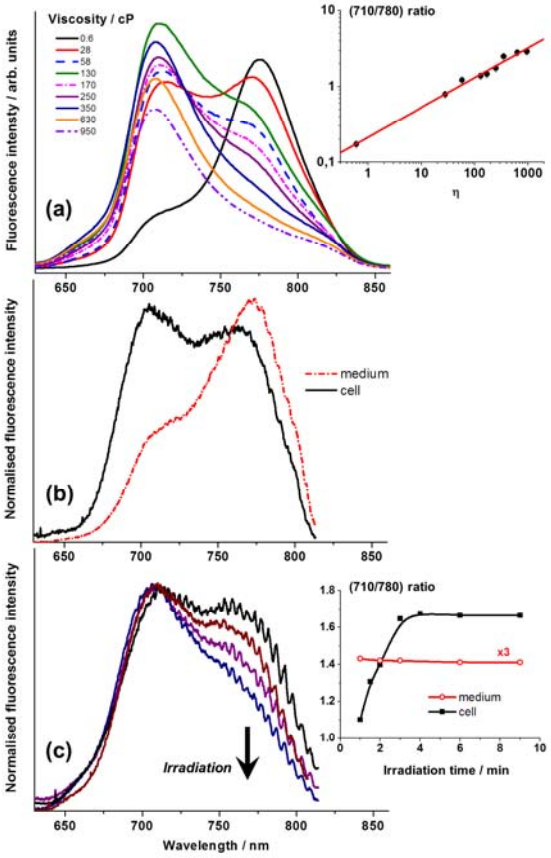
Viscosity / cP
0.6
28
58
130
170
250
350
630
950
Fluorescence intensity / arb. units
(a)
(710/780) ratio
η
Normalised fluorescence intensity
(b)
medium
cell
Normalised fluorescence intensity
(c)
Irradiation
(710/780) ratio
x3
medium
cell
Irradiation time / min
Wavelength / nm

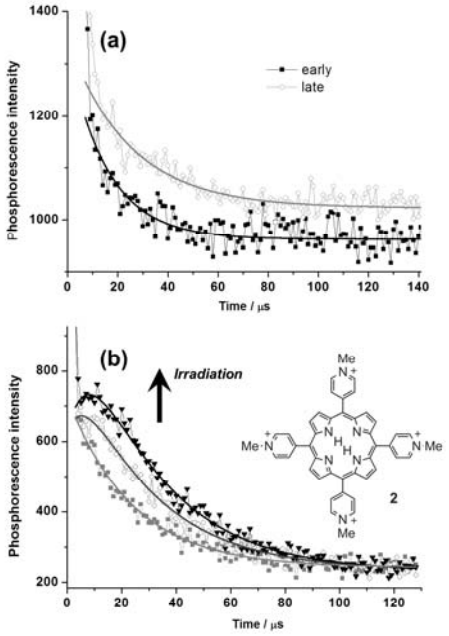
(a)
early
late
Phosphorescence intensity
Time / μs
(b)
Irradiation
Phosphorescence intensity
Time / μs
2

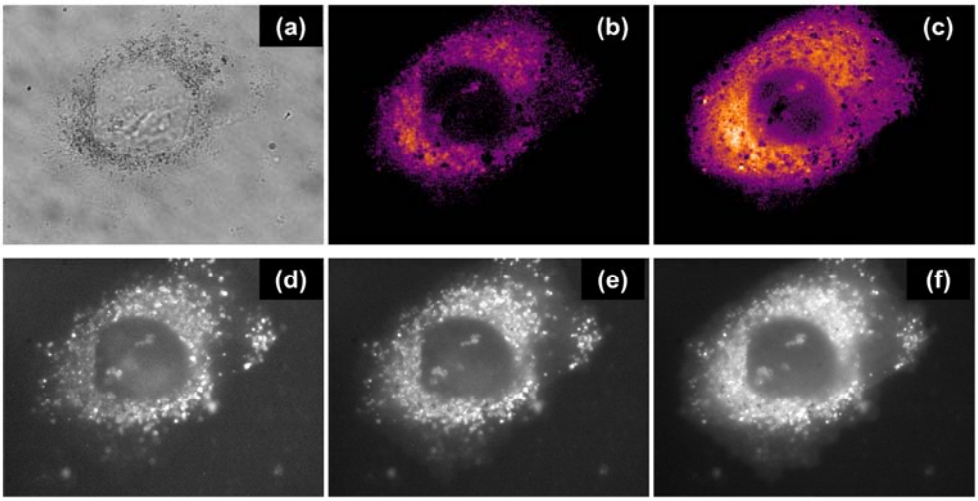
(a)
(b)
(c)
(d)
(e)
(f)